Effect of Ca Content on Properties of Extruded Mg-3Zn-0.5Sr-xCa Alloys for Medical Applications

Yajing Zhang[a]* , Wuxian Peng[a], Tingting Guo[a], Yiming Wang[a], Shuaiping Li[a]

[a]*School of Materials Science & Engineering, Northeastern University, Shenyang, China.*

Mg-3Zn-0.5Sr-xCa(wt.%) (x=0, 0.2, 0.5) alloys were fabricated by casting and hot extrusion. X-ray diffraction (XRD) and optical microscopy observation showed that the microstructure of Mg-3Zn-0.5Sr-xCa alloys was composed of α-Mg matrix and $Mg_{17}Sr_2$ phase precipitated along grain boundaries. The tensile strength of the alloy increased from 255MPa to 305MPa with increasing Ca content from 0 to 0.5wt%, but the elongation to fracture of the alloys was 19.45%, 28.7% and 15.2% respectively, indicating that coarse precipitation increased the risk of crack initiation and propagation along the grain boundaries leading to reduced ductility of Mg alloys. The polarization curves revealed that Mg-3Zn-0.5Sr-0.2Ca has the highest corrosion potential and the lowest corrosion current density indicating the optimum corrosion resistance. In cytotoxicity test, Mg-3Zn-0.5Sr-xCa alloys were harmless to mouse osteoblastic and Mg-3Zn-0.5Sr-0.2Ca alloy exhibited optimal biocompatibility.

Keywords: *Mg-Zn alloys, corrosion resistance, cytotoxicity, biocompatibility.*

1. Introduction

Magnesium alloys have attracted extensive attention for medical applications because of their good biocompatibility, biodegradability and elastic modulus similar to natural bone as orthopaedic and cardiovascular implant[1-3]. Nevertheless, traditional Mg alloys are degraded before the tissue is healed after implantation, leading to failure of the surgery, which limits the applications of the magnesium alloys to a great extent[4,5]. Alloying and deformation treatment are two methods to reduce the degradation rate of Mg alloys[6-9]. Zn, Sr and Ca are essential trace elements and non-toxic to human[10-12]. The proper amount of Zn precipitated along the grain boundaries of Mg matrix could restrict grain growth and play the dual roles of aging strengthening and solution strengthening[13,14]. Brar et al.[15] reported that when the addition of zinc is 2wt% or 4wt%, the Mg alloy has optimal mechanical and degradation properties. Sr could improve bone strength and density and indicated beneficial effects on corrosion resistance and deformability[16-19]. When Sr content is over 0.3wt%, the finer grains and more homogeneous precipitation of Mg alloys occurs. However, when the content of Sr is more than 1.2wt%, the eutectic structure with continuous network distribution appears along grain boundaries attributed to coarse grains and inferior properties. Hence, the addition of Sr in this paper is 0.5wt%. The front of solid-liquid interface generates constituent supercooling after adding Ca element, which could enhance nucleation rate and inhibit grain growth. Thereby, Ca might enhance the strength and ductility of Mg alloys. Moreover, Ca largely improves the corrosion resistance of alloys[20-22]. Comparing to as-cast Mg alloys, finer grains and preferable properties were possessed by as-extruded Mg alloys[2,10,23].

Therefore, Mg-3Zn-0.5Sr-xCa (x=0, 0.2, 0.5) alloys were fabricated through casting and hot extrusion, while the properties of the alloys were evaluated by tissue analysis, corrosion resistance and cytotoxicity tests.

2. Experimental process

The experimental raw materials were commercial pure Mg (99.99%), pure Zn (99.99%), pure Ca (99.97%) and Mg-20wt%Sr master alloy. After casting, aging treatment and extrusion, bars with a diameter as 12 mm were obtained and then were cut into 4 mm thick specimens. Specimens were polished, etched with an etchant containing 10g picric acid, 10mL acetic acid, 50mL anhydrous ethanol and 10mL distilled water. Microstructure was observed using metallographic microscope (OLTMPUS GX51) and crystallographic phase was investigated using X-ray diffraction (XRD, RIGAKU-3014). Tensile tests were carried out with a CMT5105 universal testing machine at room temperature. The tensile test specimens had a dog-bone shape with a diameter of 5mm and a gauge length of 30mm. A four-electrode cell with a sensing electrode, the specimen as a working electrode, a graphite electrode as a counter electrode and a saturated calomel electrode as a reference electrode was used for electrochemical tests. Polarization curve was measured by potentiostatic scanning at a scan rate of $5\times10^{-4}\,V\cdot s^{-1}$ and electrochemical impedance has an adopted amplitude of 5mV AC signal with test frequency at a range of $10^5\sim10^{-2}$Hz. The electrochemical corrosion test was conducted in simulated body fluid (SBF) at 37°C. Cytotoxicity assessment samples of different compositions were processed into Φ10×4mm discs and polished with metallographic sandpaper to remove scale.

*e-mail: zhangyj@smm.neu.edu.cn

Then samples were cleaned with deionized water and alcohol for 5 minutes respectively, then dried in cold air and sterilized at 121℃ for 20 minutes. Well-grown mouse osteoblasts were incubated in 96-well cell culture plate at 1×10^3 cells / 100μL in each well and cultured for 24h at 37℃ in a humidified atmosphere with 5% of CO_2, 100μl of extract or 100μl of a negative control (α-minimum Eagle's medium) could then substitute for the medium. Extracts were prepared as an extraction medium with the surface area to an extraction medium ratio 1.25cm²/ml and diluted by 100% for back-up. In this test, the cell viability was obtained by Cell Counting Kit-8(CCK8) method and the relative growth rate (RGR) was calculated. Cytotoxicity was evaluated according to the cytotoxicity evaluation criteria of ISO 10993.5: 1999[24].

3. Results and Discussion

XRD pattern (Fig. 1) show the phases of as-extruded Mg-3Zn-0.5Sr-xCa alloys consisted of α-Mg matrix and $Mg_{17}Zn_2$ intermetallic compound phase. The optical microscopy images of the microstructure of Mg-3Zn-0.5Sr-xCa alloys revealed that the addition of Ca caused grain refinement, as shown in Figures 2((a)-(c)). The Mg-3Zn-0.5Sr-0.5Ca alloy had the finest grain size and coarse precipitation. Table1 lists the mechanical properties of the Mg-3Zn-0.5Sr-xCa alloys and Table 1 shows that with addition of 0.2wt%Ca, the yield strength (YS) of the alloy decreased from 164MPa to 126MPa, but its ultimate tensile strength (UTS) remained almost unchanged and its elongation to fracture increased from 19% to 29%. With the addition of the Ca content to 0.5wt%, the YS of the Mg alloy slightly increased from 164MPa to 185MPa, and the UTS increased significantly to 305MPa, while the elongation to fracture decreased from 19% to 15%. The Mg-3Zn-0.5Sr-0.5Ca alloy had maximum UTS and YS due to its finest grain size which causes the maximum grain boundary strengthening effect as quantified by the Hall-Petch relationship. Meanwhile, the presence of a large amount of $Mg_{17}Sr_2$ intermediate phase along grain boundaries could also enhance the strength of alloys because of precipitation strengthening. However, its elongation to fracture is only 15%, which indicates that the coarse $Mg_{17}Sr_2$ particles could become the sites for crack initiation, resulting in inferior ductility of the alloys. Although the UTS of Mg-3Zn-0.5Sr-0.2Ca alloy is 257MPa, it could satisfy the mechanical performance requirements of natural bone (UTS in the range of 140-190MPa[25, 26]). On the other hand, the elongation to fracture of Mg-3Zn-0.5Sr-0.2Ca alloy

improved remarkably and reported 29%, which can decrease "Stress shielding" effects[27, 28]. Therefore, the comprehensive mechanical properties of the Mg-3Zn-0.5Sr-0.2Ca alloy are optimal for medical applications.
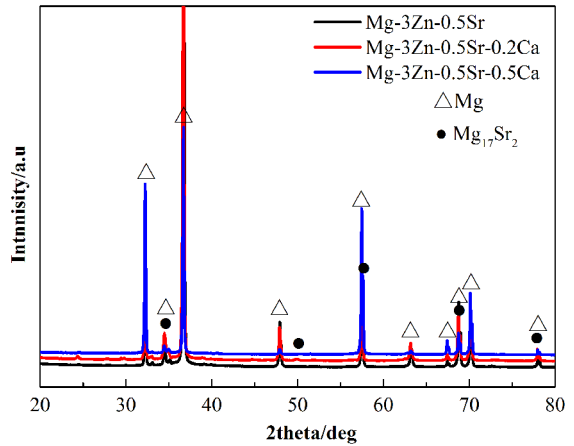

Figure 1. The XRD patterns of Mg-3Zn-0.5Sr-xCa alloys

Fig. 3 shows representative potentiodynamic polarization curves of Mg-3Zn-0.5Sr-xCa alloys in SBF solution. The corrosion potential (E_{corr}) and corrosion current density (I_{corr}) of alloys were -1.656V, -1.609V, -1.646V and 1.35×10^{-4}A·cm⁻², 1.02×10^{-4}A·cm⁻², 1.91×10^{-4}A·cm⁻² respectively with increasing Ca content from 0 to 0.5wt%. The Mg-3Zn-0.5Sr-0.2Ca alloy sample had the highest corrosion potential and the lowest corrosion current density among all the samples. Fig. 4 presents the electrochemical impedance spectroscopy (EIS) curves of the Mg-3Zn-0.5Sr-xCa alloys and curves show that the Mg-3Zn-0.5Sr-0.2Ca alloy had the largest capacitive arc diameter. Therefore, the corrosion resistance of the Mg-3Zn-0.5Sr-0.2Ca alloy is optimal according to the polarization curves and EIS curves.

$Mg_{17}Sr_2$ phase was more stable than α-Mg phase and had a higher corrosion potential[2]. With the immersion of Mg-3Zn-0.5Sr-0.2Ca alloy sample in SBF solution, $Mg_{17}Sr_2$ phase acted as cathode and the α-Mg phase acted as anode, which can form a galvanic cell to accelerate the degradation of alloys [7]. The number of precipitates observed along the grain boundaries in Mg-3Zn-0.5Sr and Mg-3Zn-0.5Sr-0.5Ca alloys were larger as compared to Mg-3Zn-0.5Sr-0.2Ca alloy, leading to a decrease in corrosion resistance. It was noticeable that Mg-3Zn-0.5Sr-0.2Ca alloy had the optimal corrosion resistance.

Table 1. The mechanical properties of Mg-3Zn-0.5Sr-xCa alloys

	Ultimate Tensile Strength /MPa	Yield Strength /MPa	Elongation /%
Natural Bone	140-190	100-190	<3
Mg-3Zn-0.5Sr	255	164	19
Mg-3Zn-0.5Sr-0.2Ca	257	126	29
Mg-3Zn-0.5Sr-0.5Ca	305	185	15

(a) Mg-3Zn-0.5Sr

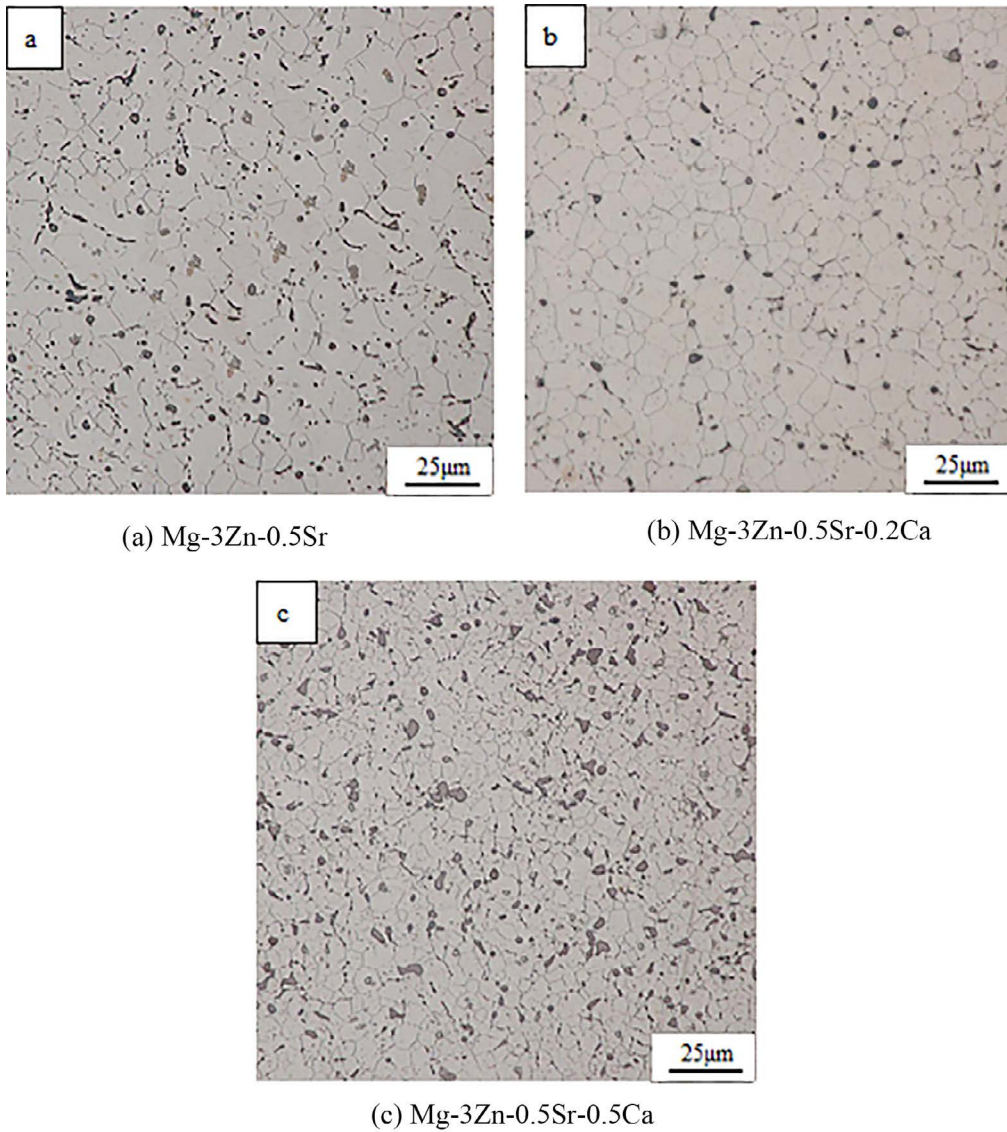(b) Mg-3Zn-0.5Sr-0.2Ca

(c) Mg-3Zn-0.5Sr-0.5Ca

Figure 2. The optical micrographs of Mg-3Zn-0.5Sr-xCa alloys perpendicular to extruded direction, (a) Mg-3Zn-0.5Sr; (b) Mg-3Zn-0.5Sr-0.2Ca; (c) Mg-3Zn-0.5Sr-0.5Ca
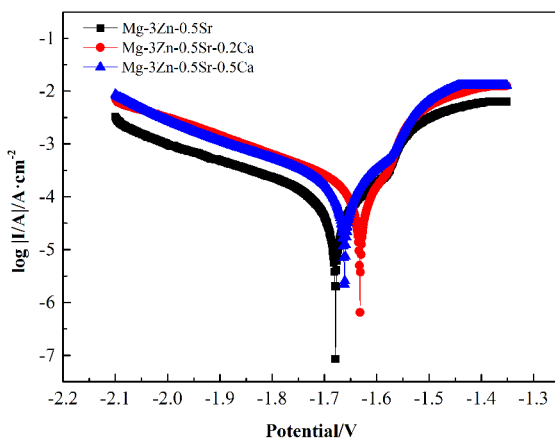

Figure 3. The polarization curves of Mg-3Zn-0.5Sr-xCa alloy samples in the SBF solution
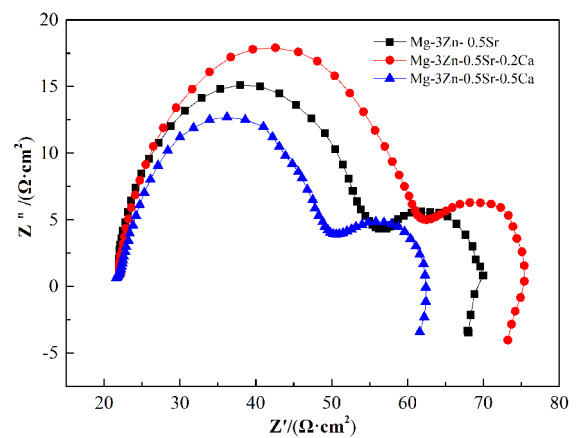
Figure 4. The electrochemical impedance spectroscopy (EIS) plot of Mg-3Zn-0.5Sr-xCa alloy samples in the SBF solution

In vitro cytotoxicity of Mg-3Zn-0.5Sr-xCa alloys were estimated by measuring the RGR of mouse osteoblasts with different concentration of extracts and negative control, as shown in Fig. 5. It could be seen that the RGR values in all extracts surpassed 100%, which indicated that the cytotoxicity of extracts was Grade 0 and satisfied the cytotoxicity requirements. Moreover, the RGR values of cells incubated in 100% extraction medium for 3 days were 136%±10%, 178%±7% and 104%±2% respectively, which revealed that Mg-3Zn-0.5Sr-0.2Ca alloy has the optimum biocompatibility. The morphologies of mouse osteoblasts cultured in extracts for 1 and 3 days were well growth and similar to that of negative control group, as shown in Fig. 6((a)-(h)). It was further demonstrated that Mg-3Zn-0.5Sr-xCa (x=0, 0.2, 0.5 wt%) alloy have good biocompatibility and could be employed as medical implants.
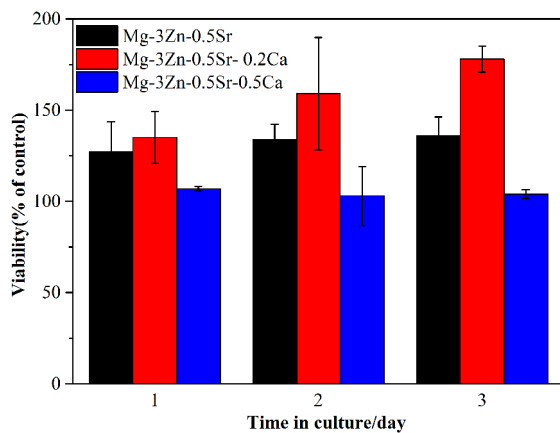

Figure 5. Mouse osteoblasts viability expressed as a percentage of the viability of cells in the control after 1, 2 and 3 days of culture in Mg-3Zn-0.5Sr-xCa alloys extraction media with 100% concentrations

4. Conclusion

Mg-3Zn-0.5Sr-xCa (x=0, 0.2, 0.5) alloys were fabricated by casting and hot extrusion. The microstructure of the alloys consisted of the α-Mg matrix and $Mg_{17}Sr_2$ particles, which were distributed along grain boundaries. The mechanical properties of alloys satisfy the requirements of Mg alloys as biomedical materials. By conducting electrochemical experiments, it has been confirmed that the Mg-3Zn-0.5Sr-0.2Ca alloy has the highest corrosion resistance. The RGR values of the alloys were all greater than 100% in extracts with diverse concentration, which revealed that Mg-Zn-Sr-xCa alloys were nontoxic for medical applications. Overall, in the present study, all three Mg alloys were promising for clinical applications and the comprehensive performance of the Mg-3Zn-0.5Sr-0.2Ca alloy was optimum.
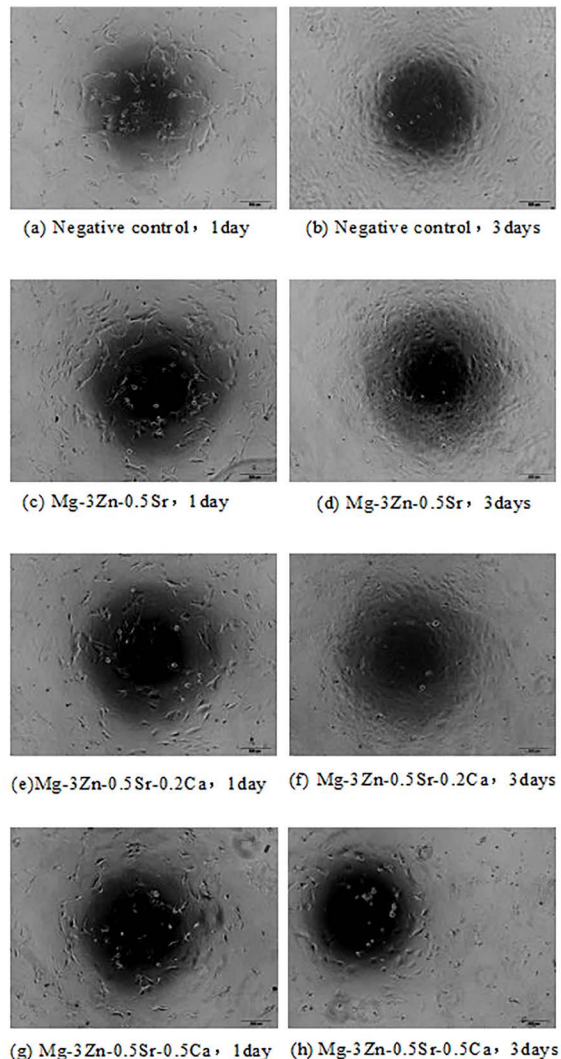

(a) Negative control，1day
(b) Negative control，3 days
(c) Mg-3Zn-0.5Sr，1 day
(d) Mg-3Zn-0.5Sr，3days
(e)Mg-3Zn-0.5Sr-0.2Ca，1day
(f) Mg-3Zn-0.5Sr-0.2Ca，3days
(g) Mg-3Zn-0.5Sr-0.5Ca，1day
(h) Mg-3Zn-0.5Sr-0.5Ca，3days

Figure 6. The morphologies of mouse osteoblasts cultured in MgZnSrCa extraction medium after 1 and 3days, (a),(c),(e)and(g) cultured for 1day; (b),(d),(f)and(h) cultured for 3 days

5. References

1. Jiang W, Cipriano AF, Tian Q, Zhang C, Lopez M, Sallee A, et al. *In vitro* evaluation of MgSr and MgCaSr alloys via direct culture with bone marrow derived mesenchymal stem cells. *Acta Biomaterialia*. 2018;72:407-423.

2. Gu XN, Xie XH, Li N, Zheng YF, Qin L. In vitro and in vivo studies on a Mg-Sr binary alloy system developed as a new kind of biodegradable metal. *Acta Biomaterialia*. 2012;8(6):2360-2374.

3. Gu X, Zheng Y, Zhong S, Xi T, Wang J, Wang W. Corrosion of, and cellular responses to Mg-Zn-Ca bulk metallic glasses. *Biomaterials*. 2010;31(6):1093-1103.

4. Purnama A, Hermawan H, Couet J, Mantovani D. Assessing the biocompatibility of degradable metallic materials: state-of-the-art and focus on the potential of genetic regulation. *Acta Biomaterialia*. 2010;6(5):1800-1807.

5. Li H, Peng Q, Li X, Li K, Han Z, Fang D. Microstructures, mechanical and cytocompatibility of degradable Mg–Zn based orthopedic biomaterials. *Materials & Design*. 2014;58:43-51.

6. Yang L, Huang Y, Feyerabend F, Willumeit R, Mendis C, Kainer KU, et al. Microstructure, mechanical and corrosion properties of Mg–Dy–Gd–Zr alloys for medical applications. *Acta Biomaterialia*. 2013;9(10):8499-8508.

7. Bornapour M, Mahjoubi H, Vali H, Shum-Tim D, Cerruti M, Pekguleryuz M. Surface characterization, in vitro and in vivo biocompatibility of Mg-0.3Sr-0.3Ca for temporary cardiovascular implant. *Materials Science & Engineering: C*. 2016;67:72-84.

8. Li Y, Wen C, Mushahary D, Sravanthi R, Harishankar N, Pande G, et al. Mg-Zr-Sr alloys as biodegradable implant materials. *Acta Biomaterialia*. 2012;8(8):3177-3188.

9. Wang HX, Guan SK, Wang X, Ren CX, Wang LG. In vitro degradation and mechanical integrity of Mg-Zn-Ca alloy coated with Ca-deficient hydroxyapatite by the pulse electrodeposition process. *Acta Biomaterialia*. 2010;6(5):1743-1748.

10. Li Z, Gu X, Lou S, Zheng Y. The development of binary Mg-Ca alloys for use as biodegradable materials within bone. *Biomaterials*. 2008;29(10):1329-1344.

11. Rosalbino F, De Negri S, Saccone A, Angelini E, Delfino S. Bio-corrosion characterization of Mg-Zn-X (X = Ca, Mn, Si) alloys for biomedical applications. *Journal of Materials Science. Materials in Medicine*. 2010;21(4):1091-1098.

12. Zhang E, Yang L, Xu J, Chen H. Microstructure, mechanical properties and bio-corrosion properties of Mg-Si(-Ca, Zn) alloy for biomedical application. *Acta Biomaterialia*. 2010;6(5):1756-1762.

13. Cipriano AF, Zhao T, Johnson I, Guan RG, Garcia S, Liu H. In vitro degradation of four magnesium-zinc-strontium alloys and their cytocompatibility with human embryonic stem cells. *Journal of Materials Science. Materials in Medicine*. 2013;24(4):989-1003.

14. Cipriano AF, Guan RG, Cui T, Zhao ZY, Garcia S, Johnson I, et al. *In vitro* degradation and cytocompatibility of Magnesium-Zinc-Strontium alloys with human embryonic stem cells. *Conference proceedings: Annual International Conference of the IEEE Engineering in Medicine and Biology Society. IEEE Engineering in Medicine and Biology Society. Annual Conference*. 2012;2012:2432-2435.

15. Brar HS, Wong J, Manuel MV. Investigation of the mechanical and degradation properties of Mg–Sr and Mg–Zn–Sr alloys for use as potential biodegradable implant materials. *Journal of the Mechanical Behavior of Biomedical Materials*. 2012;7:87-95.

16. Borkar H, Hoseini M, Pekguleryuz M. Effect of strontium on flow behavior and texture evolution during the hot deformation of Mg–1wt%Mn alloy. *Materials Science and Engineering: A*. 2012;537:49-57.

17. Wang J, Wu Y, Li H, Liu Y, Bai X, Chau W, et al. Magnesium alloy based interference screw developed for ACL reconstruction attenuates peri-tunnel bone loss in rabbits. *Biomaterials*. 2018;157:86-97.

18. Cipriano AF, Sallee A, Tayoba M, Cortez Alcaraz MC, Lin A, Guan RG, et al. Cytocompatibility and early inflammatory response of human endothelial cells in direct culture with Mg-Zn-Sr alloys. *Acta Biomaterialia*. 2017;48:499-520.

19. Guan RG, Cipriano AF, Zhao ZY, Lock J, Tie D, Zhao T, et al. Development and evaluation of a magnesium-zinc-strontium alloy for biomedical applications--alloy processing, microstructure, mechanical properties, and biodegradation. *Materials Science and Engineering: C*. 2013;33(7):3661-3669.

20. Bornapour M, Celikin M, Cerruti M, Pekguleryuz M. Magnesium implant alloy with low levels of strontium and calcium: The third element effect and phase selection improve bio-corrosion resistance and mechanical performance. *Materials Science and Engineering: C*. 2014;35:267-282.

21. Xu Z, Smith C, Chen S, Sankar J. Development and microstructural characterizations of Mg–Zn–Ca alloys for biomedical applications. *Materials Science and Engineering: B*. 2011;176(20):1660-1665.

22. Zhang B, Hou Y, Wang X, Wang Y, Geng L. Mechanical properties, degradation performance and cytotoxicity of Mg–Zn–Ca biomedical alloys with different compositions. *Materials Science & Engineering: C*. 2011;31(8):1667-1673.

23. Zhang Y, Shi G, Liu Y, Wu Q, Yang W, Zhao L. Reduction of the biodegradation rate of MgZnSrCa alloy by use of a biomimetic apatite coating. *Anti-Corrosion Methods and Materials*. 2016;63(3):226-230.

24. International Organization for Standardization (ISO). *ISO 10993-5:2009 - Biological Evaluation of Medical Devices – Part 5: Tests for in Vitro Cytotoxicity*. Geneva: ISO; 2009.

25. Staiger MP, Pietak AM, Huadmai J, Dias G. Magnesium and its alloys as orthopedic biomaterials: A review. *Biomaterials*. 2006;27(9):1728-1734.

26. Pietak A, Mahoney P, Dias GJ, Staiger MP. Bone-like matrix formation on magnesium and magnesium alloys. *Journal of Materials Science. Materials in Medicine*. 2008;19(1):407-415.

27. Salahshoor M, Guo Y. Biodegradable Orthopedic Magnesium-Calcium (MgCa) Alloys, Processing, and Corrosion Performance. *Materials (Basel)*. 2012;5(1):135-155.

28. Yang J, Cui F, Lee IS. Surface modifications of magnesium alloys for biomedical applications. *Annals of Biomedical Engineering*. 2011;39(7):1857-1871.